Received 5 March 2020; accepted 22 March 2020. Date of publication 24 March 2020; date of current version 16 April 2020.
The review of this article was arranged by Editor T.-L. Ren.

Digital Object Identifier 10.1109/JEDS.2020.2983197

Energy-Delay Sensitivity Analysis of a Nanoelectromechanical Relay With the Negative Capacitance of a Ferroelectric Capacitor

CHANKEUN YOON[1], GIHUN CHOE[2], AND CHANGHWAN SHIN[1] (Senior Member, IEEE)

1 Department of Electrical and Computer Engineering, Sungkyunkwan University, Suwon 16419, South Korea
2 School of Electrical and Computer Engineering, Georgia Institute of Technology, Atlanta, GA 30332, USA

CORRESPONDING AUTHOR: C. SHIN (e-mail: cshin@skku.edu)

This work was supported in part by the National Research Foundation of Korea (NRF) funded by the MSIP (Fundamental Technology Program) under Grant NRF-2015046617, and in part by the National Research Foundation of Korea through a grant funded by the Korean Government (MSIP) under Grant 2020R1A2C1009063.

ABSTRACT The energy-delay sensitivity of a nanoelectromechanical (NEM) relay and an NEM relay with the negative capacitance of a ferroelectric capacitor (NC + NEM relay) are theoretically investigated. The energy-delay characteristics of the NC + NEM relay deteriorate compared to those of the NEM relay when its movable beam becomes shorter/thicker than the critical beam length/thickness. The energy-delay characteristics of the NC + NEM relay (vs. the NEM relay) can be improved by increasing/decreasing the movable beam length/thickness. However, the maximum length and minimum thickness of the movable electrode are specified. This is necessary to avoid stuck-on failure. This study provides guidelines for improving the switching energy-delay characteristics and the operating voltage of the NC + NEM relay (vs. the NEM relay) by optimizing the device design variables.

INDEX TERMS Energy-delay sensitivity, ferroelectric capacitor, nanoelectromechanical relay, negative capacitance.

I. INTRODUCTION

The transistors in integrated circuits (ICs) have been aggressively scaled down to enhance the transistor performance and the functions of the ICs. However, this results in the increased off-state leakage current (I_{off}) of the transistor even when the IC transistors are turned off. The energy consumption in the off-state may drastically increase because an IC comprises billions of transistors. This hampers the scaling of the power supply voltage (V_{DD}). Therefore, an appropriate technology to reduce the I_{off} is of particular importance. I_{off} can be theoretically suppressed by (i) increasing the threshold voltage (V_{th}) or (ii) decreasing/improving the subthreshold slope (SS), which is the gate voltage (V_{GS}) that is required to increase the drain current (I_{DS}) by 10 times. However, increasing the V_{th} results in a reduced on-state drive current (I_{on}). In addition, SS is limited to 60 mV/decade at the room temperature (a.k.a, the Boltzmann limit). To address this issue, various steep switching devices, which exhibit an SS of sub-60 mV/decade, have been proposed [1]–[3]. These steep switching devices can achieve reduced I_{off} and static power consumption because their SS is less than 60 mV/decade at 300 K. Among these devices, the nanoelectromechanical (NEM) relay has received significant attention because it has almost zero SS and negligible I_{off} [4], [5]. Recently, several studies have indicated that the operating voltage and electrical characteristics of an NEM relay can be reduced/improved by connecting it in series with a ferroelectric capacitor [6], [7]. The concept of the series-connected structure, i.e., "the NEM relay + ferroelectric capacitor," originates from voltage amplification, generated by the negative capacitance (NC) phenomenon in a ferroelectric capacitor. In a previous study, the improved energy-delay properties of an NEM relay with the NC of a ferroelectric capacitor (NC + NEM relay) when compared with those

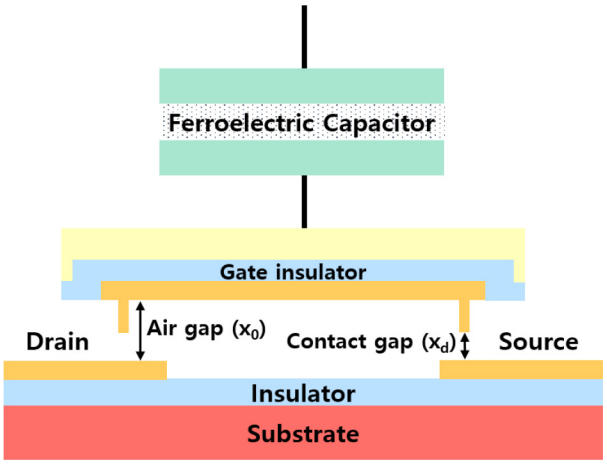

FIGURE 1. A schematic of the NC + NEM relay. A ferroelectric capacitor is connected in series to the gate electrode of the NEM relay.

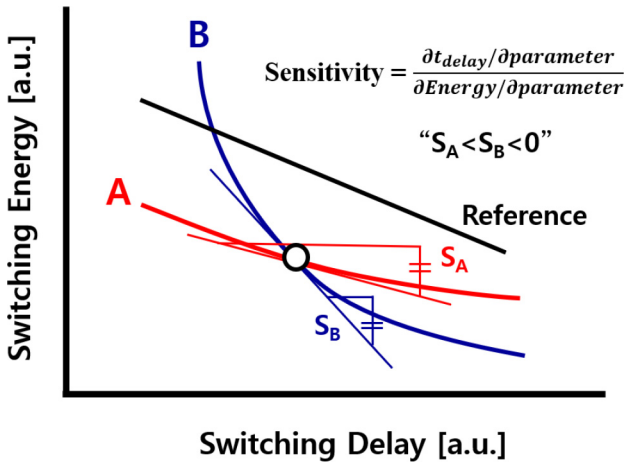

FIGURE 2. Energy-delay characteristics of two devices (i.e., A and B) with different energy-delay sensitivity.

of the NEM relay were investigated [9]. This improvement can be attributed to voltage amplification. However, there is a critical point, where the energy-delay properties of the NC + NEM relay begin to deteriorate compared to those of the NEM relay. In this study, a device design guideline is proposed to improve the energy-delay properties and operating voltage of the NC + NEM relay compared to those of the conventional NEM relay using sensitivity analysis.

II. SIMULATION METHODS

A schematic of the NEM relay connected in series to a ferroelectric capacitor (NC + NEM relay) is presented in Fig. 1. There are three main forces that control the behavior of the NEM relay, i.e., (i) the spring force (F_{spring}), which moves the movable beam away from the fixed electrode, (ii) the electrostatic force (F_{elec}), which moves the movable beam toward the fixed electrode, and (iii) the adhesion force (F_{ad}) in the contact region. If the sum of F_{elec} and F_{ad} is greater than F_{spring} (i.e., $F_{elec} + F_{ad} > F_{spring}$), the movable beam is attached to the fixed electrode, causing the abrupt flow of the current. This phenomenon is called "pull-in." However, if the sum of F_{elec} and F_{ad} is less than F_{spring} (i.e., $F_{elec} + F_{ad} < F_{spring}$), the movable beam is released from the fixed electrode, preventing the abrupt flow of the current. This phenomenon is called "pull-out." In this simulation, metal-to-metal contacts are used for obtaining low on-state resistance [9]. The adhesion force between the metal-to-metal contacts can be expressed as follows [8], [9]:

$$F_{ad}(x) = 2\gamma A_c \left(\frac{x - D_0}{{\lambda_M}^2}\right) e^{\frac{x-D_0}{\lambda_M}}, \quad (1)$$

where γ denotes the surface energy density, D_0 denotes the average atomic distance when metal-to-metal contact is formed, λ_M denotes the characteristic decay length, and x denotes the distance between the fixed electrode and the movable beam electrode. The pull-in voltage (V_{pi}) and pull-out voltage (V_{po}) of the NEM and NC + NEM relay can be expressed as follows [6]–[9]:

$$V_{pi\_NEM} = \sqrt{\frac{8k{x_0}^3}{27\varepsilon_0 A_N}}, \quad (2)$$

$$V_{po\_NEM} = \sqrt{\frac{2(x_0 - x_d)^2(kx_d - F_{ad})}{\varepsilon_0 A_N}}, \quad (3)$$

$$V_{pi\_NCNEM} = \frac{2{\alpha_N}^{EFF}}{3\sqrt{3}} \sqrt{\frac{{\alpha_N}^{EFF}}{{\beta_N}^{EFF}}}, \text{ and} \quad (4)$$

$$V_{po\_NCNEM} = \frac{{\alpha_N}^{EFF}}{\alpha_{PI}} V_{po\_NEM} - \frac{{\beta_N}^{EFF}}{{\alpha_{PI}}^3} {V_{po\_NEM}}^3, \quad (5)$$

where $\alpha_N^{EFF} = (kx_0 - F_{ad})/(k\varepsilon_0 A_N) - (-\alpha' t_{FE}/A_{FE})$, ${\beta_N}^{EFF} = 1/(2k(\varepsilon_0 A_N)^2) - \beta' t_{FE}/{A_{FE}}^3$, $\alpha_{PI} = (x_0 - x_d)/(\varepsilon_0 A_N)$, k is the spring constant of the movable beam, x_0 is the air gap, ε_0 is the dielectric constant of vacuum, A_N is the actuation area, x_d is the fabricated contact gap, t_{FE} is the thickness of the ferroelectric capacitor, A_{FE} is the area of the ferroelectric capacitor, and α' and β' are the ferroelectric anisotropy constants. In this simulation, $Sr_{0.8}Bi_{2.2}Ta_2O_9$ (SBT) is used as the ferroelectric capacitor. The electrical parameters and dimensions of the NEM relay and the ferroelectric capacitor are summarized in Table 1. In case of a clamped-clamped beam structure, the spring constant (k) can be analytically expressed as follows [10]:

$$k = 32E{W_{beam}}{t_{beam}}^3/{L_{beam}}^3, \quad (6)$$

where E is the Young's modulus of the movable beam material, W_{beam} is the beam width, t_{beam} is the beam thickness, and L_{beam} is the beam length. Poly–$Si_{0.4}Ge_{0.6}$ was selected as the beam material. Its Young's modulus (E) is 145 GPa [11]. When a voltage is applied to the NEM and NC + NEM relay, the movable beam moves according to the Newton's second law [12].

$$m\frac{d^2x}{dt^2} = \frac{\varepsilon_0 A_N V^2}{2{x_0}^2} - kx, \quad (7)$$

where m is the mass of the movable beam, x is the displacement, and V is the voltage applied to the NEM and

TABLE 1. Modeling parameters.

Symbol	Description	Unit	Value
γ	Surface energy density	J/m^2	1.6
D_0	Average atomic distance	nm	0.165
λ_M	Characteristic decay length	nm	0.1
x_0	Air gap	nm	100
x_d	Contact gap	nm	60
A_N	Actuation area	μm^2	900
A_c	Contact area	nm^2	100
t_{FE}	Ferroelectric capacitor thickness	nm	150
A_{FE}	Ferroelectric capacitor area	μm^2	2.6
α'	Ferroelectric anisotropy constant	m/F	-6.5×10^7
β'	Ferroelectric anisotropy constant	$m^5/(C^2F)$	-3.75×10^9
L_{beam}	Beam length	μm	10
t_{beam}	Beam thickness	nm	120
W_{beam}	Beam width	μm	10
ρ	Density of the beam material	kg/m^3	4,126

NC + NEM relay. The mass of the movable beam can be given as follows [10]:

$$m = 0.4\rho L_{beam} W_{beam} t_{beam}, \tag{8}$$

where ρ is the density of the beam material (herein, poly–$Si_{0.4}Ge_{0.6}$). The switching delay of the NEM relay (t_{NEM}) and the NC + NEM relay (t_{NC+NEM}) was calculated at the time at which the displacement of the movable beam (x) became equal to the contact gap (x_d). Meanwhile, the energy consumption per switching cycle (E_{switch}) can be calculated as follows [5]:

$$E_{switch} = \frac{\varepsilon_0 A_N}{x_0 - x_d} {V_{DD}}^2 \tag{9}$$

The energy-delay sensitivity with respect to the device design parameters can be defined as follows:

$$\text{Sensitivity} = \frac{\partial t_{delay}/\partial parameter}{\partial Energy/\partial parameter} \tag{10}$$

The equation above denotes how the delay reduction per energy cost can be obtained by varying the device design parameters [13]. Further, the negative correlation between the switching energy and the delay of NEM relay was previously investigated [9], [13]. When the switching energy of NEM relay increases, the switching delay decreases, and vice versa. Therefore, the energy-delay sensitivity should be a negative value in (10). Fig. 2 shows the switching energy-delay characteristics of two devices (i.e., device A and device B) with different energy-delay sensitivity. If the switching energy for both device A and device B equally increases, the switching delay of device A decreases (i.e., improves) more than that of device B. Therefore, the device A has a better switching energy-delay characteristics than the device B because the device A can more reduce its switching delay than the device B at the same cost of switching energy. In terms of switching energy-delay sensitivity, the energy-delay sensitivity of device A (S_A) is lower than that of the device B (S_B) [i.e., $S_A < S_B < 0$ in (10)]. Therefore, we can conclude that the energy-delay characteristics improve with more negative value of sensitivity. According to (2) and (6), the pull-in voltage of the NEM relay can be reduced by (i) reducing the air gap, (ii) increasing the beam length, and (iii) decreasing the beam thickness. In this study, the optimal air gap of NEM relay was initially determined. Subsequently, the energy-delay properties and operating voltage of the NEM and NC + NEM relay are compared by varying (i) the beam length and (ii) the beam thickness. The impact of variation of the device parameters (herein, the beam length and/or the beam thickness) on the operating voltage and the switching energy-delay properties of the NEM and NC + NEM relay are determined by employing a reference device, which is designed with the device parameters in Table 1.

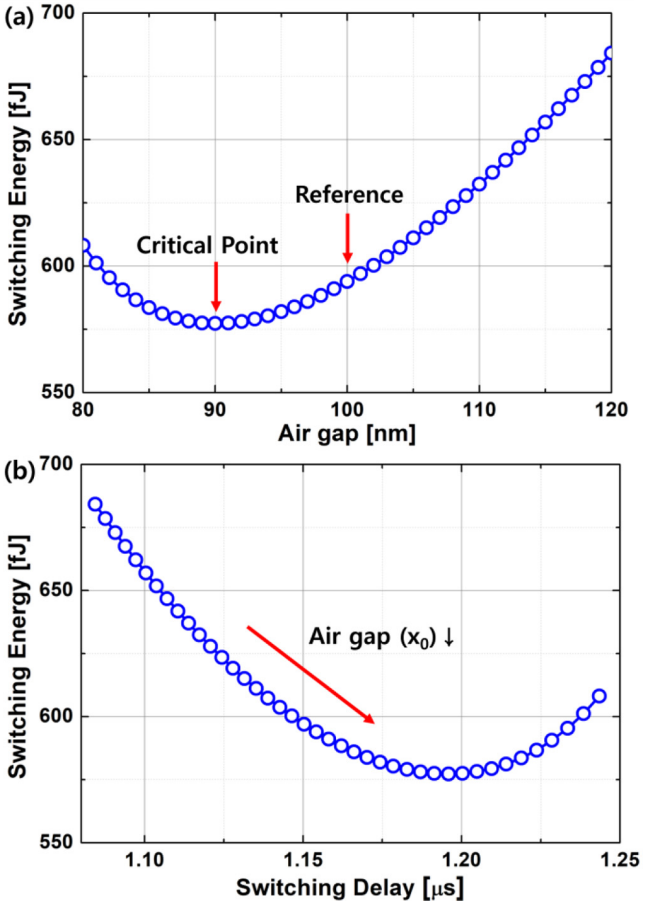

FIGURE 3. The simulated (a) switching energy vs. air gap of the NEM relay and (b) switching energy vs. delay of the NEM relay.

III. RESULTS AND DISCUSSION

A. AIR GAP (X_0)

As shown in Fig. 3(a), the switching energy decreases as the air gap of NEM relay reduces. However, below a critical air gap value (herein, $x_0 = 90$ nm), the switching energy increases as the air gap of NEM relay decreases. Similarly,

the energy-delay properties deteriorate if the air gap of NEM relay becomes smaller than the critical air gap [see Fig. 3(b)]. Herein, the critical air gap is estimated when the air gap is 1.5 times higher than the contact gap (i.e., $x_{0\_critical} = 1.5x_d$). The switching energy (E_{switch}) of NEM relay can be expressed as a function of the air gap, according to (2) and (9).

$$E_{switch} = \frac{\varepsilon_0 A_N}{x_0 - x_d} {V_{DD}}^2 = \frac{\varepsilon_0 A_N}{x_0 - x_d} {V_{pi}}^2 = \frac{8}{27} \times \frac{32 E W_{beam} {t_{beam}}^3}{{L_{beam}}^3} \times \frac{{x_0}^3}{(x_0 - x_d)} \quad (11)$$

Meanwhile, the first-order derivative and the second-order derivative of switching energy with respect to the air gap (i.e., dE_{switch}/dx_0 and $d^2E_{switch}/{dx_0}^2$, respectively) can be expressed as follows:

$$\frac{dE_{switch}}{dx_0} = \frac{8}{27} \times \frac{32 E W_{beam} {t_{beam}}^3}{{L_{beam}}^3} \times \frac{{x_0}^2 (2x_0 - 3x_d)}{(x_0 - x_d)^2} \quad (12)$$

$$\frac{d^2E_{switch}}{{dx_0}^2} = \frac{8}{27} \times \frac{32 E W_{beam} {t_{beam}}^3}{{L_{beam}}^3} \times \frac{2x_0\{\left(x_0 - \frac{3}{2}x_d\right)^2 + \frac{3}{4}{x_d}^2\}}{(x_0 - x_d)^3} \quad (13)$$

The equations above indicate that dE_{switch}/dx_0 becomes zero when $x_0 = 1.5x_d$. In (13), if the air gap (x_0) is designed to be thicker than the contact gap (x_d) (i.e., $x_0 > x_d$), then we can make the value of $d^2E_{switch}/{dx_0}^2$ to be always positive. To sum up, (i) dE_{switch}/dx_0 becomes zero if the design constraint (i.e., $x_0 = 1.5x_d$) is satisfied, and thereby, (ii) $d^2E_{switch}/{dx_0}^2$ can be positive. In Calculus, it is known that, if x is a critical point of f(x) (i.e., $df(x)/dx = 0$) and the second-order derivative of f(x) is positive (i.e., $d^2f(x)/dx^2 > 0$), f(x) has a minimum value at the x. Therefore, the switching energy should be minimized if the design constraint of $x_0 = 1.5x_d$ is satisfied. Because the NEM relay has the minimum switching energy when $x_0 = 1.5x_d$, the air gap is designed to be 90nm-thick (if the contact gap is given as 60 nm). Subsequently, by modulating the beam length and thickness, the switching energy-delay properties and operating voltage of NC + NEM relay vs. NEM relay can be quantitatively compared and discussed.

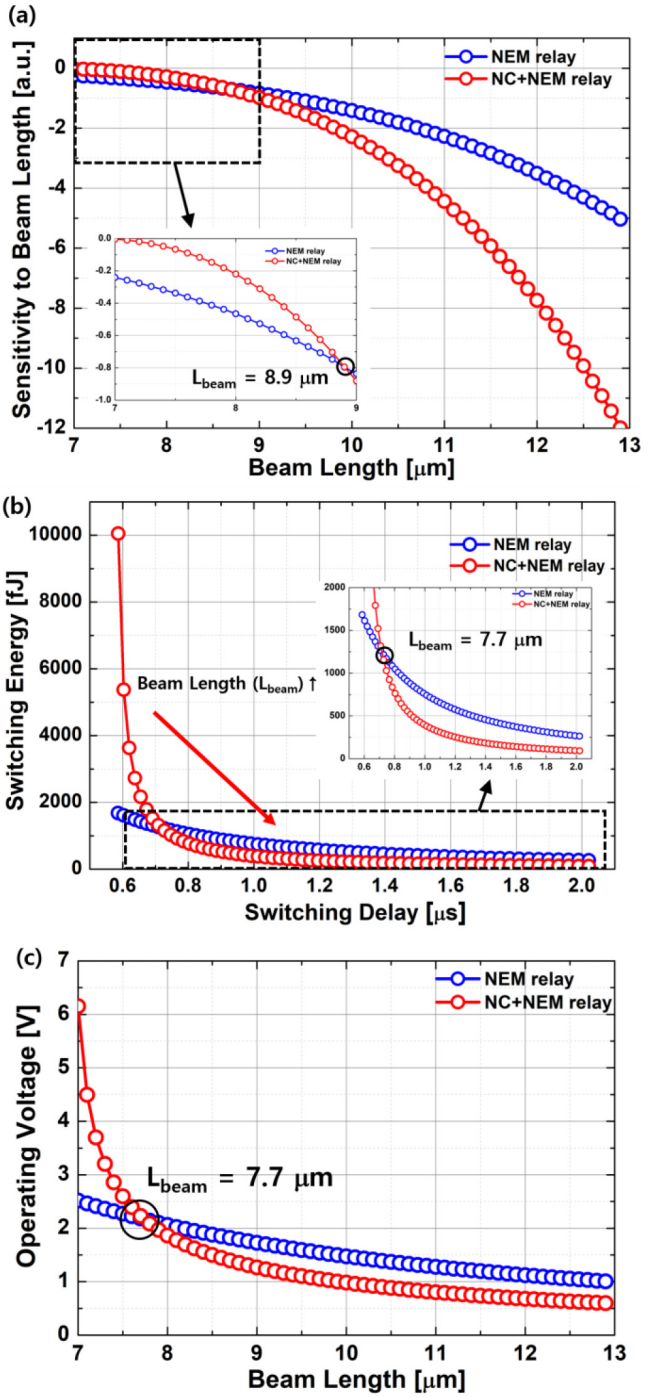

FIGURE 4. (a) Estimated sensitivity to beam length vs. the beam length, (b) switching energy vs. delay, and (c) operating voltage of NEM relay and NC + NEM relay vs. the beam length.

B. BEAM LENGTH (L_{BEAM})

Once the air gap of NEM relay was determined, the beam length of the reference device was varied by ±30%. Subsequently, the electrical characteristics of the NEM and NC + NEM relay were compared. The switching energy-delay sensitivity to the beam length versus the beam length of the NEM and NC + NEM relay is illustrated in Fig. 4(a). This figure indicates that the sensitivity of the NC + NEM relay is improved compared to that of the NEM relay with an increase in the beam length. Specifically, the switching sensitivity to the beam length of the NC + NEM relay is improved by 142.37% compared to that to the beam length of the NEM relay when the beam length becomes 13 μm. Further, as the beam length decreases, the switching sensitivity to the beam length of the NC + NEM relay worsens. The inset in Fig. 4(a) shows that the switching energy-delay sensitivity to the beam length of the NC + NEM relay becomes worse than that of the NEM relay when the

beam length becomes shorter than 8.9 μm. The switching energy-delay properties of the NEM and NC + NEM relay are shown in Fig. 4(b). When the beam length becomes shorter than 8.9 μm, the switching energy-delay properties of NC + NEM relay degrade more than those of NEM relay since the sensitivity to beam length of the NC + NEM relay worsens than that of the NEM relay. Eventually, the energy-delay properties of NC + NEM relay worsen than those of the NEM relay when the beam length becomes shorter than 7.7 μm. The operating voltages of the NEM and NC + NEM relay, which decrease with an increase in the beam length, are shown in Fig. 4(c). However, as the beam length is increased to improve the performance of the NEM and NC+NEM relay, the spring constant reduces according to (6). If the spring constant reduces even further to cause the spring restoring force to become smaller than the adhesion force (i.e., $kx_d < F_{ad}$), a stuck-on failure occurs. In this case, the electrodes of the movable beam and the fixed electrode do not fall apart [14]. Thus, there is a lower limit for the spring constant, which means that there is an upper limit for the beam length. The maximum value of the beam length is 16 μm, which is the value observed when the spring restoring force becomes equal to the adhesion force.

C. BEAM THICKNESS (T_{BEAM})

The beam thickness of the reference device was adjusted by ±30%, and the electrical characteristics of the NEM and NC + NEM relay were compared. Fig. 5(a) illustrates the switching energy-delay sensitivity to the beam thickness versus the beam thickness of the NEM and NC + NEM relay. This figure indicates that the switching energy-delay sensitivity to the beam thickness of the NC + NEM relay improves compared to that of the NEM relay with decreasing the beam thickness. Specifically, the sensitivity to the beam thickness of the NC + NEM relay is improved by 163.26% compared to that of the NEM relay when the beam thickness is 84 nm. However, as the beam thickness increases, the switching sensitivity to the beam thickness of the NC + NEM relay worsens. The inset in Fig. 5(a) indicates that the switching energy-delay sensitivity to the beam thickness of the NC + NEM relay worsens than that of the NEM relay when the beam thickness becomes thicker than 134 nm. The switching energy-delay properties of the NEM and the NC + NEM relay are shown in Fig. 5(b). When the beam thickness becomes thicker than 134 nm, the switching energy-delay properties of the NC + NEM relay deteriorates more than those of NEM relay since the sensitivity to the beam thickness of the NC + NEM relay worsens than that of the NEM relay. Eventually, the energy-delay properties of the NC + NEM relay worsens than those of the NEM relay when the beam thickness becomes thicker than 154 nm. Fig. 5(c) indicates the operating voltages of the NEM and NC + NEM relay, which decrease as the beam thickness decreases. However, as the beam thickness decreases to

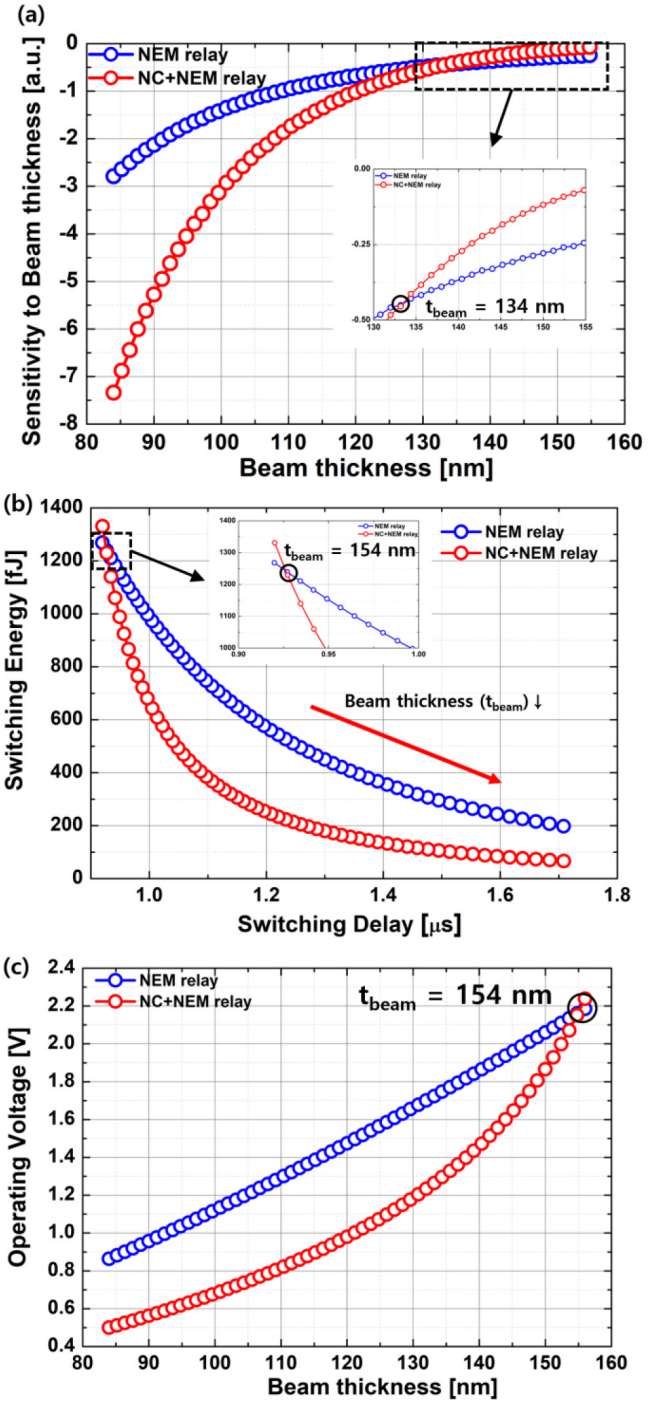

FIGURE 5. (a) Estimated sensitivity to beam thickness vs. beam thickness, (b) switching energy vs. delay, and (c) operating voltage of NEM relay and NC + NEM relay vs. beam thickness.

improve the performances of the NEM and NC+NEM relay, the spring constant reduces according to (6). If the spring constant reduces even further to cause the spring restoring force to become smaller than the adhesion force (i.e., $kx_d < F_{ad}$), a stuck-on failure occurs. Therefore, there is a lower limit for the spring constant, which means that there is a lower limit for the beam thickness. The minimum

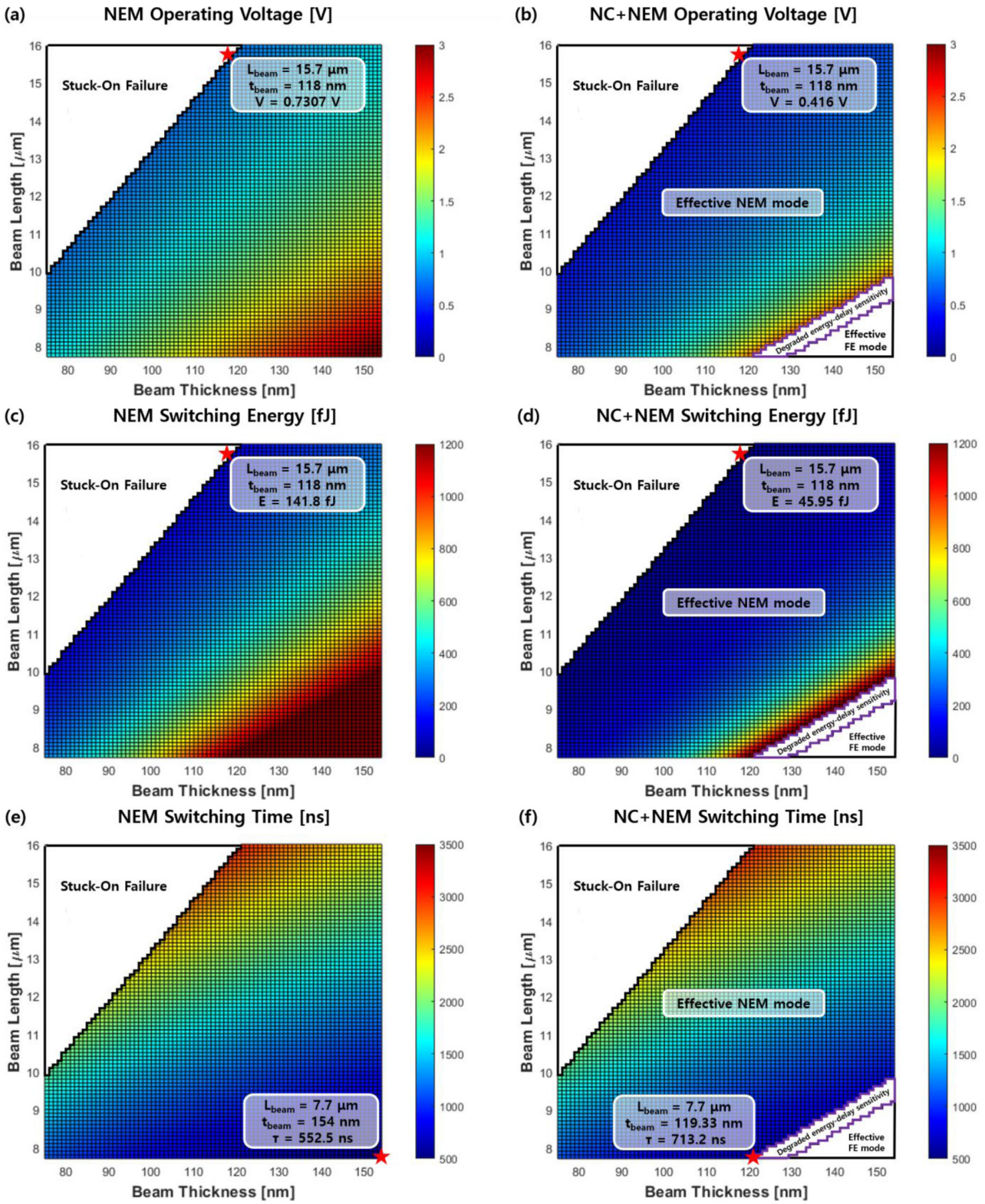

FIGURE 6. Estimated (a) operating voltage of NEM relay and (b) NC + NEM relay, switching energy of (c) NEM relay and (d) NC + NEM relay, and switching delay of (e) NEM relay and (f) NC + NEM relay.

value of the beam thickness is 75 nm, which is the value observed when the spring restoring force becomes equal to the adhesion force.

D. BEAM LENGTH (L_{BEAM}) & BEAM THICKNESS (T_{BEAM})

The performance of the NEM and NC + NEM relay improves when the beam length increases and/or the beam

thickness decreases. Furthermore, there is a maximum value for the beam length (herein, 16 μm) and a minimum value for the beam thickness (herein, 75 nm) to avoid the occurrence of stuck-on failure. We have varied both (i) the beam length of the reference device in the range of 7.7 μm $\leq L_{beam} \leq$ 16 μm (i.e., from the value at which the switching energy-delay properties of the NC + NEM relay deteriorate, compared to those of the NEM relay to the maximum value) and (ii) the beam thickness of the reference device in the range of 75 nm $\leq t_{beam} \leq$ 154 nm (from the minimum value to the value at which the switching energy-delay properties of the NC + NEM relay deteriorate compared to those of the NEM relay). As the beam length and thickness are varied together, the spring constant is correspondingly varied. Therefore, in certain regimes, the spring restoring force becomes smaller than the adhesion force, causing the stuck-on failure (i.e., $kx_d < F_{ad}$). We marked the regimes where the NEM relay and the NC + NEM relay do not operate due to the stuck-on failure in Fig. 6.

The NC + NEM relay can be operated in two different modes, i.e., (i) effective NEM mode and (ii) effective ferroelectric (FE) mode; the NC + NEM relay in effective NEM mode operates as a conventional NEM relay. If α_N^{EFF} and β_N^{EFF} are positive, the NC + NEM relay are working in effective NEM mode. To improve the electrical characteristics, the NC + NEM relay needs to operate in effective NEM mode [6]. Therefore, we found the regime where the NC + NEM relay operates in an effective NEM mode. The purple-colored box in Fig. 6 represents the regime where the energy-delay properties of the NC + NEM relay deteriorate compared to those of the NEM relay due to the degraded energy-delay sensitivity. This regime is not desirable for the NC + NEM relay to improve its energy-delay properties compared to those of the NEM relay. In summary, except for the regime where (i) a stuck-on failure occurs, (ii) the NC + NEM relay operates in the effective FE mode, and (iii) the energy-delay properties of the NC + NEM relay deteriorate compared to those of the NEM relay, the switching energy-delay properties and the operating voltage of NEM and NC + NEM relay are compared.

Figs. 6(a) and 6(b) indicate the operating voltage of NEM and NC + NEM relay, respectively, according to the variation of the beam length and thickness. These results verify that the operating voltage decreases as the beam length increases and the beam thickness decreases. In particular, the minimum operating voltage of the NEM/NC + NEM relay is obtained when L_{beam} = 15.7 μm, t_{beam} = 118 nm. The minimum operating voltage of the NC + NEM relay was 43.07% lower than that of the NEM relay. Overall, the operating voltage of the NC + NEM relay is lower than that of the conventional NEM relay.

The variation in the switching energies of the NEM and the NC + NEM relay according to the variation of the beam length and thickness is presented in Fig. 6(c) and 6(d), respectively. Similar to the operating voltage, the results verify that the switching energy decreases as the beam length increases and the beam thickness decreases. The minimum switching energy of the NEM/NC + NEM relay is obtained when the L_{beam} = 15.7 μm, t_{beam} = 118 nm. The minimum switching energy of the NC + NEM relay is 67.6% smaller than that of the NEM relay. Overall, the switching energy of the NC + NEM relay is lower than that of the conventional NEM relay.

The operating mechanism of NC + NEM relay can be given as follows: (i) the voltage is simultaneously applied to the movable electrode of the NEM relay and the top electrode of the NC + NEM relay and (ii) a voltage is applied to the movable electrode of the NEM relay after the polarization switching of the ferroelectric capacitor when the voltage is applied to the top electrode of the NC + NEM relay. In the former case, the switching delay of the NC + NEM relay is similar to that of the NEM relay. However, in the latter case, the switching delay of the NC + NEM relay is the sum of the switching delay of the NEM relay and the ferroelectric polarization switching time. The switching delays of the NEM and NC + NEM relay are illustrated in Fig. 6(e) and 6(f), respectively. Herein, 200 ps of the ferroelectric polarization switching time [15] is added to the switching delay of the NC + NEM relay to quantitatively estimate the worst switching delay of the NC + NEM relay. The simulation results indicate that the beam length should be decreased and that the beam thickness should be increased. This is necessary to decrease the switching delays of the NEM and NC + NEM relay. Furthermore, the minimum switching delay of the NEM relay is obtained when L_{beam} = 7.7 μm, t_{beam} = 154 nm. However, in case of the NC + NEM relay, it operates in the effective FE mode when L_{beam} = 7.7 μm, t_{beam} = 154 nm. Instead, the minimum switching delay of the NC + NEM relay is obtained when L_{beam} = 7.7 μm, t_{beam} = 119.33 nm. The minimum switching delay of the NC + NEM relay is 29.45% slower than that of the NEM relay due to the ferroelectric polarization switching time. However, in the effective NEM mode, it was observed that the identical switching delay of NEM relay and NC + NEM relay can be achieved by slightly increasing the operating voltage of the NC + NEM relay (i.e., reducing the voltage amplification effect in ferroelectric capacitor). Even in this case, the operating voltage and switching energy of the NC + NEM relay is observed to be still smaller than those of the NEM relay.

IV. CONCLUSION

The energy-delay sensitivity analysis of the NC + NEM relay indicated that its energy-delay characteristics were worse than those of the NEM relay when the beam length/thickness became shorter/thicker than its critical length/thickness. Further, the performance of the NC + NEM relay could be improved compared to that of the NEM relay by increasing the beam length and decreasing the beam thickness.

REFERENCES

[1] W. Y. Choi, B.-G. Park, J. D. Lee, and T.-J. K. Liu, "Tunneling field-effect transistors (TFETs) with subthreshold swing (SS) less than 60 mV/dec," *IEEE Electron Device Lett.*, vol. 28, no. 8, pp. 743–745, Aug. 2007, doi: 10.1109/LED.2007.901273.

[2] N. Shukla *et al.*, "A steep-slope transistor based on abrupt electronic phase transition," *Nat. Commun.*, vol. 6, p. 7812, Aug. 2015, doi: 10.1038/ncomms8812.

[3] S. Salahuddin and S. Datta, "Use of negative capacitance to provide voltage amplification for low power nanoscale devices," *Nano Lett.*, vol. 8, no. 2, pp. 405–410, Dec. 2007, doi: 10.1021/nl071804g.

[4] R. Nathanael, V. Pott, H. Kam, J. Jeon, and T.-J. K. Liu, "4-terminal relay technology for complementary logic," in *Proc. IEEE Int. Electron Devices Meeting*, Baltimore, MD, USA, 2009, pp. 9.4.1–9.4.4, doi: 10.1109/IEDM.2009.5424383.

[5] V. Pott, H. Kam, R. Nathanael, J. Jeon, E. Alon, and T.-J. K. Liu, "Mechanical computing redux: Relay for integrated circuit applications," *Proc. IEEE*, vol. 98, no. 12, pp. 2076–2094, Dec. 2010, doi: 10.1109/JPROC.2010.2063411.

[6] M. Masuduzzaman and M. A. Alam, "Effective nanometer air-gap of NEMS devices using negative capacitance of ferroelectric materials," *Nano Lett.*, vol. 14, no. 6, pp. 3160–3165, May 2014, doi: 10.1021/nl5004416.

[7] K. Choe and C. Shin, "Adjusting the operating voltage of an nano-electromechanical relay using negative capacitance," *IEEE Trans. Electron Devices*, vol. 64, no. 12, pp. 5270–5273, Dec. 2017, doi: 10.1109/TED.2017.2756676.

[8] K. Choe and C. Shin, "Impact of negative capacitance on the energy-delay property of an electromechanical relay," *Jpn. J. Appl. Phys.*, vol. 58, no. 5, Apr. 2019, Art. no. 051003, doi: 10.7567/1347-4065/ab0ee7.

[9] I.-R. Chen, C. Qian, E. Yablonovitch, and T.-J. K. Liu, "Nanomechanical switch designs to overcome the surface adhesion energy limit," *IEEE Electron Device Lett.*, vol. 36, no. 9, pp. 963–965, Sep. 2015, doi: 10.1109/LED.2015.2463119.

[10] W. Y. Choi, "Design and scaling of nano-electro-mechanical non-volatile memory (NEMory) cells," *Current Appl. Phys.*, vol. 10, no. 1, pp. 311–316, Jan. 2010, doi: 10.1016/j.cap.2009.06.014.

[11] H. Kam and F. Chen, *Micro-Relay Technology for Energy Efficient Integrated Circuits*. Springer, 2015.

[12] G. M. Rebeiz, *RF MEMS: Theory, Design and Technology*. Hoboken, NJ, USA: Wiley, 2003.

[13] H. Kam, T.-J. K. Liu, V. Stojanovic, D. Markovic, and E. Alon, "Design, optimization, and scaling of MEM relay for ultra-low-power digital logic," *IEEE Trans. Electron Devices*, vol. 58, no. 1, pp. 236–250, Jan. 2011, doi: 10.1109/TED.2010.2082545.

[14] C. Qian, A. Peschot, I.-R. Chen, Y. Chen, N. Xu, and T.-J. K. Liu, "Effect of body biasing on the energy-delay performance of logic relay," *IEEE Electron Device Lett.*, vol. 36, no. 8, pp. 862–864, Jun. 2015, doi: 10.1109/LED.2015.2441116.

[15] J. Li, B. Nagaraj, H. Liang, W. Cao, C. H. Lee, and R. Ramesh, "Ultrafast polarization switching in thin-film ferroelectric," *Appl. Phys. Lett.*, vol. 84, no. 7, p. 1174, Dec. 2003, doi: 10.1063/1.1644917.